Proceedings of the Institution of Mechanical Engineers, Part D: Journal of Automobile Engineering
Volume 231, Issue 10, 2017, pp. 1353-1373
DOI:10.1177/0954407016672591

KINETIC ENERGY STORAGE USING A DUAL BRAKING SYSTEM FOR UNMANNED PARALLEL HYBRID ELECTRIC VEHICLE.

Piranavan Suntharalingam*, John T Economou**†, K. Knowles**

**Aeromechanical Systems Group

Centre for Defence Engineering

Cranfield University

Defence Academy of the United Kingdom

Shrivenham

SN6 8LA

*Formerly a Cranfield University PhD student.

†*Corresponding author: j.t.economou@cranfield.ac.uk*

Suntharalingam P, Economou JT, Knowles K. (2016) Kinetic energy storage using a dual braking system for unmanned parallel hybrid electric vehicle. Proceedings of the Institution of Mechanical Engineers, Part D: Journal of Automobile Engineering. Online first 06/11/2016. **doi:10.1177/0954407016672591**

Proc. ImechE, Part D: Journal of Automotive Engineering Accepted: 23rd Aug 2016
Corresponding Author: John Economou: *j.t.economou@cranfield.ac.uk*

ABSTRACT

In this paper a novel regenerative dual braking strategy is proposed for utility/goods delivery unmanned vehicles in public roads, which improves the regenerative energy capturing ability and consequently improves the fuel use of parallel hybrid power train configurations for land unmanned vehicles where the priority is not comfort but extending the range. Furthermore, the analysis takes into account the power handling ability of the electric motor and the power converters. In previous research a plethora of regenerative braking strategies is shown, for this paper the key contribution is that the vehicle electric regeneration is related to a fixed braking distance in relation to the energy storage capabilities specifically for unmanned utility type land vehicles where passenger comfort is not a concern but pedestrian safety is of critical importance. Furthermore, the vehicle's power converter capabilities facilitate the process of extending the braking time via introducing a variable deceleration profile. The proposed approach has therefore resulted in a regenerative algorithm which improves the vehicle's energy storage capability without considering comfort since this analysis is applicable to unmanned vehicles. The algorithm considers the distance as the key parameter, which is associated to safety, therefore it allows the braking time period to be extended thus favouring the electric motor generation process while sustaining safety. This method allows the vehicle to brake for longer periods rather than short bursts hence resulting in a more effective regeneration with reduced use of the dual (i.e. caliper/stepper motor brake system). The regeneration method and analysis is addressed in the following paper sections. The simulation results show that the proposed regenerative braking strategy has improved significantly the energy recapturing ability of the hybrid power train configuration. The paper is also supported with experimental data that verify the theoretical development and the simulation results. The two strategies developed and implemented are Constant Braking Torque (CBT) and Constant Braking Power (CBP). Both methods were limited to a fixed safety-based distance. Overall the results demonstrate that the CBT method results in better energy-based savings.

Proc. ImechE, Part D: Journal of Automotive Engineering Accepted: 23rd Aug 2016

Corresponding Author: John Economou: *j.t.economou@cranfield.ac.uk*

1 INTRODUCTION

Hybrid vehicles and their variants have been described extensively in Shuang et al.[1] and Khaligh et al.[2] clearly showing the key benefits for adopting these into the market place worldwide. Hybrid vehicles with plug-in options offer more flexibility to the user. In [2], it is reported that Hybrid vehicle solutions in the future can become very competitive especially as their electric driving range extends. Hence, the motivation behind this paper is to offer this opportunity to hybrid vehicles by extending their overall range through better kinetic energy capturing. Regenerative braking is investigated in Kumar et al.[18] however that paper focuses on adjusting the braking effort from both the conventional braking and the regenerative braking so that the driver feels no difference with reference to the braking method. However in this paper we consider unmanned vehicles whereby no humans are on board therefore the braking effort can be achieved with a major priority on energy capturing rather than passenger comfort. When a conventional internal combustion vehicle is braking, the kinetic energy is normally dissipated as heat in the disk brakes, suspension and tyres. This paper is focused towards enhancing the recovery of kinetic energy for a parallel hybrid electric vehicle. Therefore, the challenge for the regenerative braking process is the design of an effective and efficient kinetic energy capturing system which maximizes the electrical energy which can be stored. In Zhang [3], the importance of the energy that can be captured from a vehicle is highlighted and linked to electric or hybrid vehicles simply because these have already on-board the necessary technology to harness this energy. In Wang et al.[4] the authors analysised the benefits, in terms of fuel burnt for hybrid vehicles when kinetic-energy-based regeneration was used, thus showing a regenerative torque optimization strategy.

Furthermore in the literature a hydraulic module is proposed by Yeo et al.[5] for a parallel hybrid electric vehicle. The battery State of Charge (*SoC*), motor capacity and vehicle velocity were considered as the decision-making variables for the regenerative braking algorithms. In Bhangu et al.[6] a non-linear observer solution was shown for predicting the state-of-charge of lead-acid batteries within the context of hybrid vehicles. Battery model complexity was sustained at reasonable levels while a Kalman filter was used to compensate for the battery model discrepancies. The paper in [6] also used an Extended Kalman filter for the state of health of the battery while operating with a hybrid vehicle under various demands. The latter indicates the importance of capturing energy while also sustaining this function over long periods of time in practical systems. Physics-based regenerative braking and a control strategy for a parallel hybrid electric vehicle is presented in Panagiotidis et al.[7], where the model has been developed in MATLAB, SIMULINK

Corresponding Author: John Economou: *j.t.economou@cranfield.ac.uk*

and STATEFLOW. A parametric analysis approach was used to illustrate the trade-off involved in component sizing in order to enhance the regenerative energy. A comprehensive analysis for brake system design and force distribution between the front and rear axles is presented in Wong [8]. Miller [9] considers application-based analyses on series and parallel braking strategy. The series-braking strategy is proposed for a series hybrid and electric vehicle while the parallel-braking strategy is for a parallel hybrid electric vehicle. Mietal[10] considers the feasibility of employing the electric motor in the propulsion system to achieve antilock braking performance without the involvement of a conventional antilock braking system. Indeed most of these works focus on achieving better regenerative braking efficiency while ensuring acceptable driving comfort and braking safety. The research, analysis and simulation, and consequently experimental data, in the present paper were focused towards developing a new braking strategy, whereby the regenerative energy capturing capability can be increased so that hybrid vehicles can benefit more from the energy captured during regeneration.

The primary objective of a vehicle's braking system is to ensure firstly a safe breaking capability. When a vehicle is decelerating with a very high decelerating ratio, this could result in passenger discomfort and/or mechanical transmission system premature ageing. Therefore the approach in this paper is to set a minimum braking distance (effectively maximum deceleration ratio). Furthermore, the algorithm would also need to be capable of achieving a maximum deceleration (emergency braking scenario). Statistical data on typical deceleration ratios, obtained from Paredes et al.[13] , are summarised in Table 1. The deceleration ratio will be determined by the expected braking distance of the vehicle. In addition drivability is a desired factor, highly linked to the deceleration ratio of the vehicle.

Deceleration rate	Statistic percentage
$\leq 0.2\ g$	80%
$\leq 0.25\ g$	90%
$\leq 0.3\ g$	95%
$\leq 0.35\ g$	99%

Table 1: General statistics on urban driving deceleration rate of vehicles, (Extracted from Bray et al. [11])

Table 1: General statistics on urban driving deceleration rate of vehicles, (Extracted from Bray et al. [11])

According to [8], the maximum achievable deceleration (α) can be given by $\frac{\alpha}{g} < \mu$ where μ is the coefficient of road adhesion. Therefore, μ is the determining factor for the maximum deceleration ratio and a typical value of μ is 0.85. Consequently, the maximum achievable deceleration ratio will be 0.85 g. However, in practice the deceleration ratio is determined by the unmanned vehicle brake pedal request.

Corresponding Author: John Economou: *j.t.economou@cranfield.ac.uk*

Since for the road unmanned vehicle, pedestrian safety is the primary concern the algorithm's design priority is biased towards the safest braking distance. When the vehicle is braking, the propulsion system cuts off the power supply to the drive train. Therefore, the only available energy at the starting point of the braking is the vehicle's kinetic energy. On the other hand, energy conservation is the function of the braking where the kinetic energy of the vehicle is dissipated mainly as heat (in conventional vehicles). The hardware architecture proposed in this paper consists of a hybrid braking solution; one which consists of:

(a) a conventional braking system and
(b) a regenerative energy capturing system working in parallel.

In order to shorten the braking distance, a hybrid brake system (electric motor and friction brake pad in the electric and hybrid electric vehicles) will generate a negative torque to oppose the vehicle's movement. External forces, such as aerodynamic drag and rolling resistance, depend upon the gradient, the terrain and the speed and all contribute towards reducing the braking distance of the vehicle. For electric and hybrid electric vehicles the negative torque generated by the electric motor depends on vehicle speed, the SoC availability of the battery, and the rated torque speed/efficiency characteristic of the motor.

2 PROBLEM FORMULATION

The braking distance is a critical factor for a safe vehicle when operating on public roads. Generally the percentage share of the electric propulsion system in parallel hybrid electric vehicle regenerative braking is less than 40 percent [9], therefore the maximum demanded negative (braking) torque can partially be satisfied by the electric generator alone. Thus, the energy recapturing ability of a parallel hybrid power train topology is less substantial than for series hybrid and electric topologies. Normally, the electric motors are of a greater power capacity for Series Hybrid Electric Vehicles (SHEV) when compared to Hybrid Parallel Electric Vehicles (HPEV).

Because emergency vehicle braking happens rapidly, vehicles with regeneration capability do require having also mechanical brakes too. Thus reducing the regeneration motor size to a practical physical size and acceptable power ratings for energy savings. As a result of these design motor (sizing) constraints between the hybrid architectures and the electric motor (propulsion), the inevitable need of the mechanical braking system is essential to handle the negative torque demand of the braking requirement for the case of HPEV. Below a certain vehicle speed the motor will not generate sufficient voltage to charge the battery. Although very efficient boost-up converters can be utilized their efficiency at low RPM will offer minimum advantages. Therefore from an enegy and cosequently algorithmic point of view, the mechanical braking should be minimized at the high-speed braking requirement thus enhancing the regenerative energy capturing process, (typically regeneration is better at higher speeds).

Corresponding Author: John Economou: *j.t.economou@cranfield.ac.uk*

This also implies that electrical braking should be employed for most of the braking period. Thus, increasing the vehicle's braking period while maintaining the same braking distance (safety constraint), will allow the electric braking system to increase the quantity of the regenerative energy. Consequently the regenerative energy can be obtained when the braking ratio is within the maximum and minimum deceleration ratios. The proposed method is developed and analysed in this paper by both mathematical and computer simulation in the following sections. Furthermore the work is also supported from an experimental breaking rig and experimental data which have verified the algorithm.

3 VEHICLE HYBRID ARCHITECTURE

Figure 1 shows a schematic diagram of the regenerative braking system, with the power flow and signal flow directions, of the proposed parallel hybrid electric vehicle. This uses, a four-wheel-drive parallel hybrid power train configuration integrated with an IC engine and an electric motor. There are two electric clutches (clutch 1 and clutch 2) joining the power generators with the propulsion power transmission system. Moreover the mechanical braking system is coupled with the power transmission system. Therefore, depending on the brake demand, and other conditions, a combination of the mechanical and the regenerative braking system can be activated independently. Expected braking requirement, $SoC(t)$ of the battery, speed of the vehicle are fed into the controller to perform the braking algorithm. According to the decision made by the controller, an appropriate braking sequence will be triggered to enhance the regenerative energy.

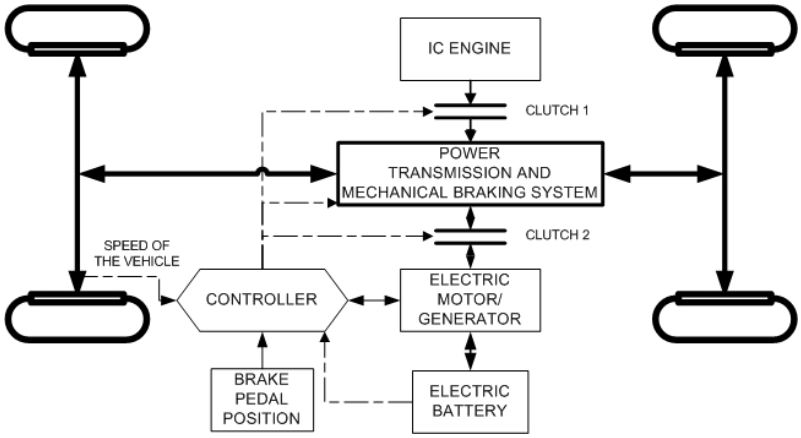

Figure 1: Propulsion and regenerative braking system of a four-wheel-drive parallel hybrid electric vehicle with representation of power flow and signal flow directions Suntharalingam [12].

3.1 DYNAMICS OF THE GROUND VEHICLE BRAKING AND MATHEMATICAL MODELING

Corresponding Author: John Economou: *j.t.economou@cranfield.ac.uk*

Braking is a life-critical requirement which is heavily legislated. Hence, when the conventional braking is complemented also by the vehicle propulsion system understanding how these two methods can co-exist becomes also a priority. Therefore, intensive efforts have been made by transportation authorities around the world towards ensuring improvement of braking performance in automobiles. While sustaining vehicle braking safety, this paper attempts to maximise the energy captured thus offering together with safe braking also an environmentally-friendly regenerative solution. The dual braking system architecture used is shown in Figure 2.

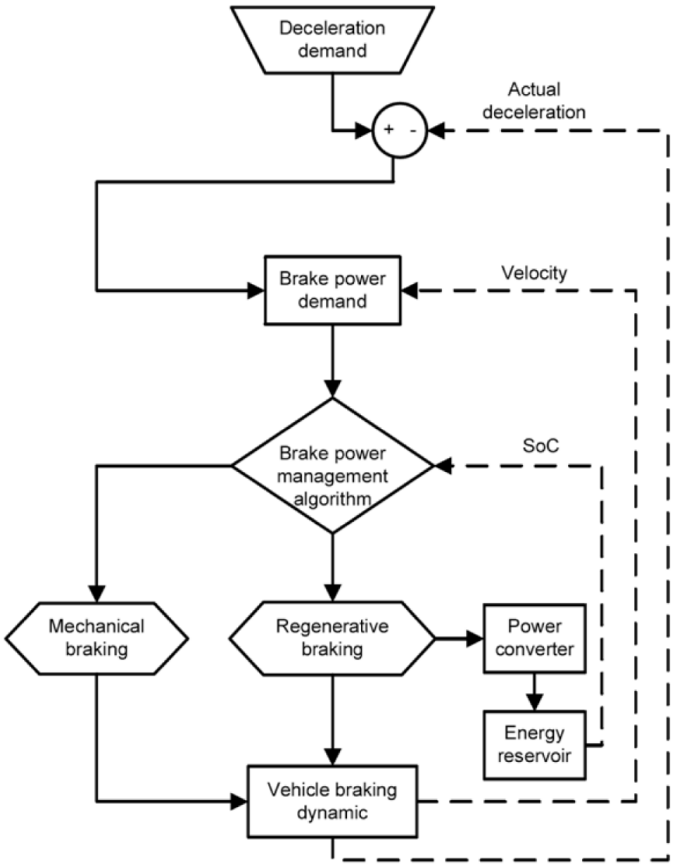

Figure 2. Dual Braking Contextual Diagram

In order to improve the braking performance and to minimize the braking distance, an analysis of the braking dynamics is presented next and correlated to the capture of the kinetic regeneration energy. In particular this section is addressing the mathematical modelling of the braking dynamics of a two-axle vehicle.

Corresponding Author: John Economou: *j.t.economou@cranfield.ac.uk*

3.1.1 BRAKING CHARACTERISTICS OF A TWO AXLE VEHICLE

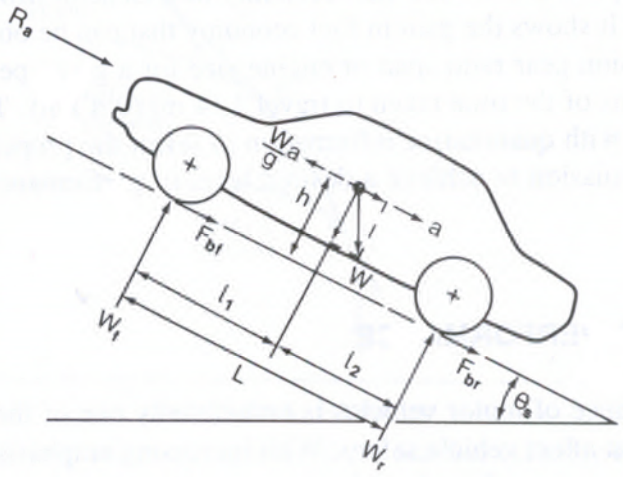

Figure 3: Forces acting on a two-axle vehicle during braking

The braking force based on the vehicle shown in Figure 3. exerted on the wheel is given from:

$$F_b = \frac{T_b - \sum I\alpha_{an}}{r} \qquad \textbf{(1)}$$

Forces such as aerodynamic resistance, ground resistance, grade resistance and transmission resistance also affect the braking performance of the vehicle and these are captured in Equation 2. The resultant braking force F_{res} can be written as [2]:

$$F_{res} = F_b + f_r.W.\cos\theta_s + R_a \pm W.\sin\theta_s \qquad \textbf{(2)}$$

In order to maintain proper contact with the ground to prevent wheel slip, the normal load acting on the wheels is related to the braking force for the individual wheel sets (front and rear). Therefore when the vehicle is braking, the normal load acting on the front axle W_f (front wheels) and rear axle W_r (rear wheels) can be given has Equations 3 and 4,

$$W_f = \frac{1}{L}[W.l_2 + h(a.W/g - R_a \pm W.\sin\theta_s)] \quad \textbf{(3)}$$

$$W_r = \frac{1}{L}[W.l_1 - h(a.W/g - R_a \pm W.\sin\theta_s)] \quad \textbf{(4)}$$

Where a is the deceleration ratio of the vehicle.

When the vehicle is braking on a flat terrain, the dynamic force equilibrium in the horizontal direction can be given by:

$$F_b + f_r.W = F_{bf} + F_{br} + f_r.W = a.W/g - R_a \quad \textbf{(5)}$$

Where F_{bf} and F_{br} are the braking force action on front and rear wheels. From Equations 3, 4 and 5 W_f and W_r are reduced to:

$$W_f = \frac{1}{L}[W.l_2 + h(F_b + f_r.W)] \quad \textbf{(6)}$$

$$W_r = \frac{1}{L}[W.l_1 - h(F_b + f_r.W)] \quad \textbf{(7)}$$

From Equations 6 and 7, the maximum braking force distribution on the front and rear tyres can be expressed as $F_{bf(\max)}$ and $F_{br(\max)}$, where:

$$F_{bf(\max)} = \mu.W_f = \frac{\mu.W}{L}[l_2 + h(\mu + f_r)] \quad \textbf{(8)}$$

$$F_{br(\max)} = \mu.W_r = \frac{\mu.W}{L}[l_1 - h(\mu + f_r)] \quad \textbf{(9)}$$

Therefore, by adding Equations (8) and (9) the total maximum braking force $\mu.W$ can be obtained for the specific vehicle. (Note that the power transmission system has a connection with only the rear axle.) Therefore, when the vehicle is decelerating, the braking force that can be supplemented by the electric generator:

$$F_{generator}(t) \subseteq F_{generator(\max)} \subseteq F_{br(\max)} \quad \textbf{(10)}$$

The front wheel braking force will be given by the mechanical brake system and eventually it will be unrecovered energy loss.

Similar theory can be applied to a front-wheel-drive vehicle, where the force that can be effectively used for regenerative energy conversion will be,

$$F_{generator}(t) \subseteq F_{generator\,(\max)} \subseteq F_{bf\,(\max)} \qquad \textbf{(11)}$$

For a four-wheel-drive hybrid power train configuration we have the flexibility to gain greater energy recovery than the front- or rear-wheel-drive vehicles. Where the maximum braking force that can be used for the regenerative energy conversion will be,

$$F_{generator}(t) \subseteq F_{generator\,(\max)} \subseteq \mu.W \qquad \textbf{(12)}$$

The research in this paper is considering a four-wheel-drive parallel hybrid electric vehicle. The resulting state space equation for the deceleration ratio can be written, therefore, as:

$$\frac{dv(t)}{dt} = -\frac{1}{M}\left\{F_a + F_g + k_1(t).F_{mech} + k_2(t).F_{motor} + OF\right\} \qquad \textbf{(13)}$$

The energy of the vehicle and the fractional energy distribution can be obtained from (13) and is given by,

$$\frac{1}{2}.M.(V_{t=t_s})^2 = \int_{t=t_s}^{t=t_f} (F_a + F_g + k_1(t).F_{mech} + k_2(t).F_{motor}).v(t).dt + OE \qquad \textbf{(14)}$$

Since F_a and F_g are the external forces acting on the vehicle, by adjusting the value of $k_1(t)$ and $k_2(t)$, the deceleration ratio of the vehicle can be determined. A limitation of the operational characteristic of the electric motor, (F_{motor} is a function of the motor power and rpm) and therefore its output is saturated to practical operational levels. However, F_{mech} is significantly higher compared to the motor force and is within a practical sense unlimited. Therefore, when the unmanned vehicle is required to brake hard thus maximizing the deceleration ratio, the value of $k_1(t)$ and $k_2(t)$ will be adjusted accordingly from the proposed regenerative algorithm. However, in

order to maximize the regenerative energy captured from the vehicle braking process, the mechanical brake should be decoupled ($k_1(t)$ = 0) from the braking system. Consequently when this occurs, it reduces the deceleration ratio.

However F_{motor} depends on the hybridization factor. When the vehicle's electric propulsion power increases in the power train system, this would result in a larger electric motor. The advantage is the capturing of a larger negative torque, which will allow more regenerative energy while maintaining a safe braking distance. When F_{motor} increases, then the motor will produce more current within a short period of time and it can be challenging to accumulate this in the electric battery. Therefore, for such cases a significant amount of the recaptured energy has to be dissipated as heat at the brake resistor.

Another important constraint is that below a certain velocity (rpm of the motor), the regenerative braking efficiency drops rapidly. For a parallel hybrid vehicle F_{motor} will be relatively small because of the hybridization factor (in general, electric motor : IC engine= 0.4 : 0.6). Due to the safe braking distance requirement, the involvement of the mechanical braking is ultimately significant for the parallel hybrid electric vehicle architecture.

Next the regenerative energy captured is derived (property 1).

Corresponding Author: John Economou: *j.t.economou@cranfield.ac.uk*

PROPERTY 1:

The regenerative energy that can be captured by the vehicle is given by

$$E_{regn} = \sum_{i=1}^{n} P_{regn}(t_i)\Delta t = \sum_{i=1}^{n} \frac{1}{2} m(2U - (2i-1)a\Delta t)a\Delta t - \sum_{i=1}^{n} P_{mech}(t_i)\Delta t - \sum_{i=1}^{n} P_{others}(t_i)\Delta t \quad \textbf{(15)}$$

PROOF:

$$v(t) = U - at$$

$$KE(t) = \frac{1}{2} m(v(t)^2)$$

According to the conservation of energy

$$E_{regn} + E_{mech} + E_{others} = \frac{1}{2} m(U_{t=t_s}{}^2)$$

$E_{regn}(t) = \int_{t=t_s}^{t=t_f} P_{regn}(t)dt \cong P_{regn}(t)\Delta t$, for a small time interval Δt . Where $t_f = t_s + \Delta t$

Similarly E_{mech} and E_{others} can be written in the same format. Therefore for a small time interval Δt , the energy equation can be written as,

$$P_{regn}(t)\Delta t + P_{mech}(t)\Delta t + P_{others}(t)\Delta t = \frac{1}{2} m(u(t)^2 - (u(t) - a\Delta t)^2)$$

$$P_{regn}(t)\Delta t + P_{mech}(t)\Delta t + P_{others}(t)\Delta t = \frac{1}{2} m(2u(t) - a\Delta t)a\Delta t$$

$$P_{regn}(t)\Delta t = \frac{1}{2} m(2u(t) - a\Delta t)a\Delta t - P_{mech}(t)\Delta t - P_{others}(t)\Delta t$$

Let us assume the braking time interval T can be written as $T = n\Delta t$, $n, \Delta t > 0$,

Therefore

At $t = t_0$ energy available at the vehicle is: $\frac{1}{2} m(U^2)$

At $t = t_1 = \Delta t$ $\quad P_{regn}(t_1)\Delta t = \frac{1}{2} m(2U - a\Delta t)a\Delta t - P_{mech}(t_1)\Delta t - P_{others}(t_1)\Delta t$

At $t = t_2 = 2\Delta t$ $\quad P_{regn}(t_2)\Delta t = \frac{1}{2} m(2U - 3a\Delta t)a\Delta t - P_{mech}(t_2)\Delta t - P_{others}(t_2)\Delta t$

Similarly at any intermediate time $t = t_i = i\Delta t$, $i > 0$ the regenerative energy can be written as,

$$P_{regn}(t_i)\Delta t = \frac{1}{2} m(2U - (2i-1)a\Delta t)a\Delta t - P_{mech}(t_i)\Delta t - P_{others}(t_i)\Delta t$$

$$E_{regn} = \sum_{i=1}^{n} P_{regn}(t_i)\Delta t = \sum_{i=1}^{n} \frac{1}{2} m(2U - (2i-1)a\Delta t)a\Delta t - \sum_{i=1}^{n} P_{mech}(t_i)\Delta t - \sum_{i=1}^{n} P_{others}(t_i)\Delta t$$

In order to increase the regenerative energy, $\sum_{i=0}^{n} P_{mech}(t_i)\Delta t$, $\sum_{i=1}^{n} P_{others}(t_i)\Delta t$ should be minimized.

PROPERTY 2:

The distance traveled by the vehicle can be given by:

$$S_{braking} = \sum_{i=1}^{n} s(t_i) = \sum_{i=1}^{n} \frac{1}{2}(2U - (2i-1)a\Delta t)\Delta t \qquad \textbf{(16)}$$

PROOF:

The distance traveled by the vehicle can be given by

$$s(t) = Ut - \frac{1}{2}at^2$$

At $t = t_0$ $\quad s(t_0) = 0$

At $t = t_1 = \Delta t$ $\quad s(t_1) = \frac{1}{2}(2U - a\Delta t)\Delta t$

At $t = t_2 = 2\Delta t$ $\quad s(t_2) = \frac{1}{2}(2U - 3a\Delta t)\Delta t$

Similarly at any time interval $t = t_i = i\Delta t$, $i > 0$ the distance traveled by the vehicle can be given by

$$s(t_i) = \frac{1}{2}(2U - (2i-1)a\Delta t)\Delta t$$

Therefore the total distance traveled within the braking time interval can be given by,

$$S = \sum_{i=1}^{n} s(t_i) = \sum_{i=1}^{n} \frac{1}{2}(2U - (2i-1)a\Delta t)\Delta t$$

In order to increase the quantity of regenerative energy E_{regn} for a particular braking distance S, the time interval n or acceleration a should be dynamically changed. Moreover, since $P_{regn}(t_i)\Delta t$ is limited by the rated power output of the motor generator, whenever

$\frac{1}{2}m(2U - (2i-1)a\Delta t)a\Delta t \geq P_{regn}(t_i)\Delta t$, then the mechanical brake should be activated to fulfill the demand requirement. Therefore, the algorithm is designed to increase the time interval n by dynamically changing the value of a, which will minimize the mechanical braking losses, which can be effectively recaptured. The demanded braking distance S,

$S = \sum_{i=1}^{n} s(t_i) = \sum_{i=1}^{n} \frac{1}{2}(2U - (2i-1)a\Delta t)\Delta t$, where $S_{\min} < S < S_{\max}$

The energy recaptured by the vehicle is:

$$\left(E_{regn}\right)_{\max} = \left\{\sum_{i=1}^{n} P_{regn}(t_i)\Delta t\right\}_{\max} = \sum_{i=1}^{n} \frac{1}{2} m(2U - (2i-1)a\Delta t)a\Delta t - \left\{\sum_{i=1}^{n} P_{mech}(t_i)\Delta t\right\}_{\min} - \left\{\sum_{i=1}^{n} P_{others}(t_i)\Delta t\right\}_{\min}$$

As discussed earlier, in section 1, the braking sequence strongly influences the efficiency of the regenerative braking process. We recall that the value of $k_1(t)$ and $k_2(t)$ are the internal determining factors for the deceleration ratio and braking distance of the vehicle. Moreover when $k_1(t)$) becomes zero (i.e. no mechanical braking, just all-electric braking and $k_2(t)$ become one, then both the recaptured energy and braking distance are increased. For the shortest braking distance, $k_1(t)$ should be adjusted while maintaining $k_2(t)$ as a maximum (i.e. a mix of mechanical braking and all-electric braking).

Based on these important braking coefficients the regenerative energy management algorithm is designed to enhance the energy-recapturing ability of the vehicle. This involves a strategy that for a safe braking distance minimizes the mechanical braking while maximizing the electric braking, thus increasing the braking time without compromising the safe set braking distance. This method is highly advantageous for the architecture of an hybrid electric vehicle topology. In the following section the regenerative energy management algorithm is designed and discussed.

3.1.2 REGENERATIVE ENERGY MANAGEMENT ALGORITHM

The regenerative (braking) torque is a function of the vehicle battery SoC and the unmanned vehicle braking demand. The Regenerative Energy Management Algorithm (REMA) is designed by incorporating brake pedal position and SoC of the battery as the control variables.

$$T_{regn} = f(B\_P_{position}(t), SoC_{energy\_storage}(t), V_{vehicle}(t)) \qquad \textbf{(17)}$$

The typical decision-making procedure and the control sequence is depicted in Figure 4.

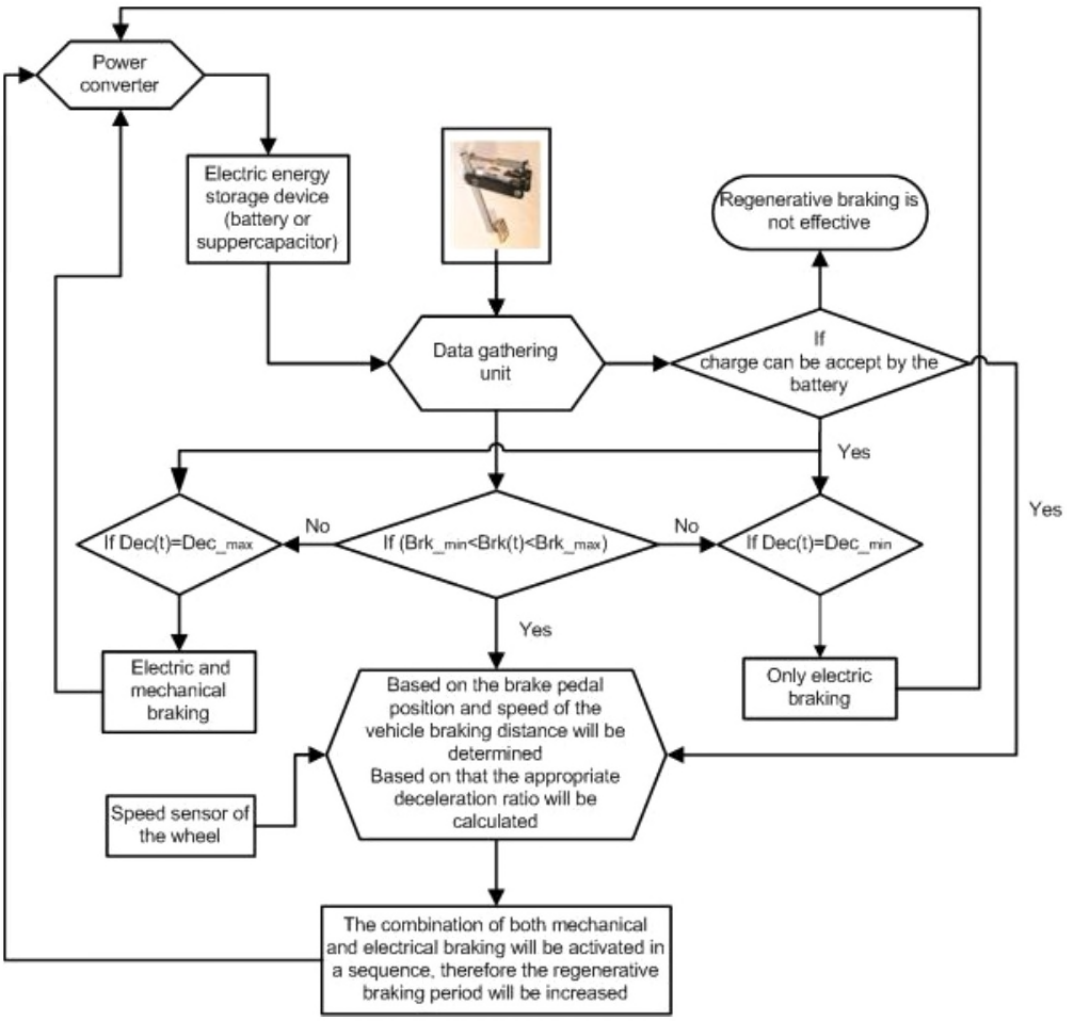

Figure 4: Decision-making and control procedure of the proposed regenerative braking strategy, [12].

Initially the state information obtained from the brake pedal position sensor and the SoC measurement sensors are both conveyed to the data gathering unit. Based on the status of the SoC of the energy storage device, the initial decision will be taken by the controller; either the electric motor can be employed for the braking or simply the mechanical brake.

If the SoC(t) of the energy storage device is below the allowable maximum limit (SoC_max) of the energy storage device, then the remaining procedures will be carried out, otherwise only the mechanical brake will be employed for the braking. Therefore the initial condition, which needs to be satisfied by the system to continue the regeneration will be:

Corresponding Author: John Economou: *j.t.economou@cranfield.ac.uk*

If ($SoC(t) < SoC\_\max$) then continue.

If this condition is not satisfied by the vehicle system, then the required braking torque demand will be supplied only from the mechanical braking system.

$$B\_Torque(t) = k(t)(Me\_T_{\max}) \text{ Where } 0 < k(t) \le 1$$

If the first condition is fulfilled by the system, then a secondary step is checked: the brake pedal position will be used in order to identify the demanded deceleration ratio. As illustrated in section 3.1.1, the brake pedal position also relates to the upper and lower braking ratio limits. The proposed algorithm is targeted to enhance the regenerative braking efficiency, when the demanded deceleration ratio is mainly within the predetermined boundaries (i.e. maximum and minimum deceleration ratio). Moreover the primary requirement is to ensure safe braking. Hence, the unmanned vehicle demands are essentially mapped to different deceleration rates. In addition to this, the algorithm takes into account the relatively low power sharing percentage of the electric propulsion system (for the parallel hybrid electric vehicle architecture) when compared to a series hybrid. Hence, the algorithm is aware that the negative torque requirement for the vehicle braking scenarios cannot be satisfied by the electric motor alone Yeo et al.[5], at all times. Regeneration normally is more effective at medium to high speeds. For cases whereby smooth braking demands are required without reaching a zero velocity electric regeneration could be used. However the proposed algorithm is mainly focusing towards reaching a final vehicle zero velocity hence mechanical braking needs to be also applied alongside the regenerative braking.

The mathematical representations of the different braking scenarios have been defined and are categorized as shown next.

$$B\_Torque(t) = \begin{cases} k_1(t)Mo\_T_{\max} \\ k_1(t)(Mo\_T_{\max}) + k_2(t)(Me\_T_{\max}) \end{cases} \quad \textbf{(18)}$$

The electric motor generator is functioning as a motor for the propulsion phase and as a generator for the braking phase. Therefore, the value of $k_1(t)$ will vary within $-1 \le k_1(t) \le 1$. Nevertheless, since there is no motoring action taking place in the braking vehicle phase, the value of $k_1(t)$ will vary within $0 \le k_1(t) \le 1$ during braking. Moreover for the mechanical braking the value of $k_2(t)$ will vary within $0 \le k_2(t) \le 1$, where, $B\_Torque(t)$ is the required braking torque to satisfy the unmanned vehicle's demand at time t. In fact these torque requirements will be a subset of the electric motor torque and

combination of electric motor and mechanical torque. In order to enhance the regenerative energy capturing ability, the electric motor will be given the priority, however if the torque demand cannot be fulfilled by the electric motor alone, then the mechanical braking system also assists the braking phase.

4 SIMULATION RESULTS

In order to firstly validate the proposed algorithm, a computer-based vehicle model is simulated in the MATLAB-Simulink environment. It has been assumed that the vehicle is braking on a flat road, therefore the gravity force is not considered. The specification of the vehicle and the allowable maximum and minimum deceleration ratios are shown in Table 2.

Mass of the vehicle	1200 kg
Aerodynamic drag coefficient	3
Hybridization factor (electrical: mechanical)	0.4:0.6
Maximum deceleration ratio	0.82g
Minimum deceleration ratio	0.14g

Table 2: Technical specification of the parallel hybrid electric vehicle [12].

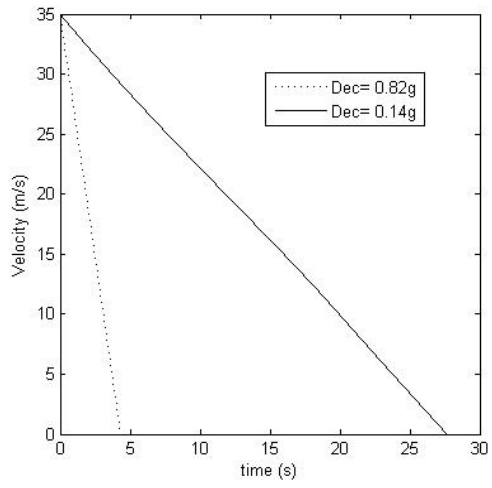

Figure 5: Velocity time graph for pure regeneration and minimum distance braking.

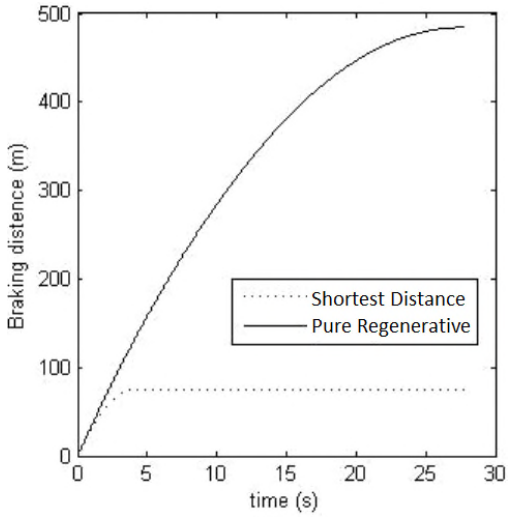

Figure 6: The distance travelled by the vehicle wrt time.

The velocity time graph for the two extreme braking (pure regenerative braking and minimum distance

braking) and the respective braking distances are shown in Figure 5 and Figure 6, respectively. When the braking distance of the vehicle is between these two different distances, then different ratios of k_1 and k_2 will achieve the objective with different levels of energy recapturing. Therefore, in order to increase the regenerative energy, the ratio of k_1 and k_2 should be optimized accordingly. Initially the simulation has been carried out with the fixed k_1 and k_2 values. It has been assumed that the vehicle is decelerating from 35m/s speed. The obtained result is given in Figure7 (constant deceleration ratio).

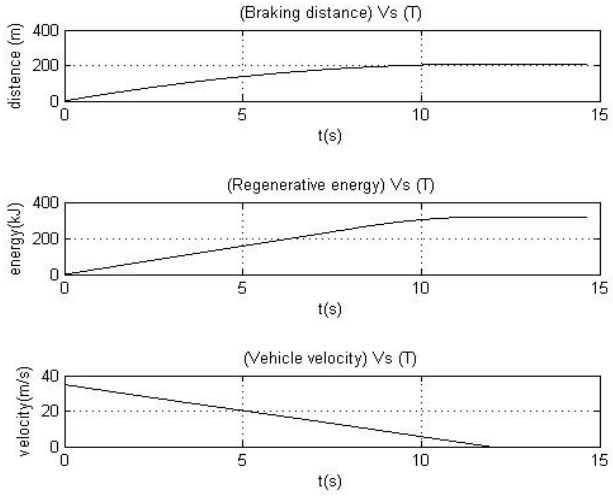

Figure 7: Case (a) - Braking distance, captured regenerative energy and the vehicle velocity for constant deceleration ratio are shown with respect to time (Initial vehicle velocity is 35m/s) [12].

In order to increase the regenerative energy efficiency the simulation has been carried out with a variable deceleration ratio for the same braking distance (approximately 200m). The algorithm manages to adjust the deceleration in case (b), so that the regenerative braking time increases (having the same braking distance as case (a)). It results in an increase of the regenerative energy for case (b), when compared with the constant deceleration ratio, case (a). The results obtained from the improved energy regeneration are shown in Figure 8 (variable deceleration ratio).

Corresponding Author: John Economou: *j.t.economou@cranfield.ac.uk*

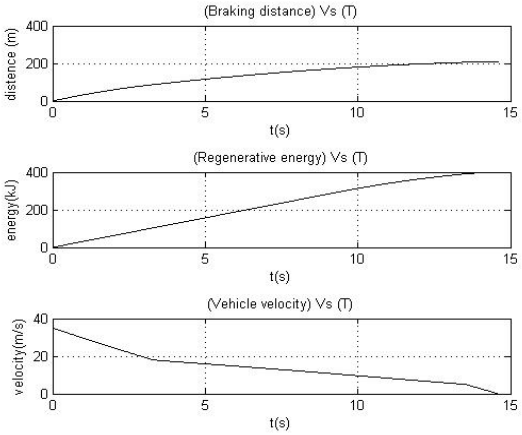

Figure 8: Case (b) - Braking distance, captured regenerative energy and the vehicle velocity variations for the variable deceleration ratio are shown with respect to the time (Initial vehicle velocity is 35m/s) [12].

A more comprehensive set of simulation results is summarized in Figure 9. The deceleration ratio and the energy recapturing ability is shown together with the percentage benefits of the variable deceleration braking compared with the constant-deceleration braking.

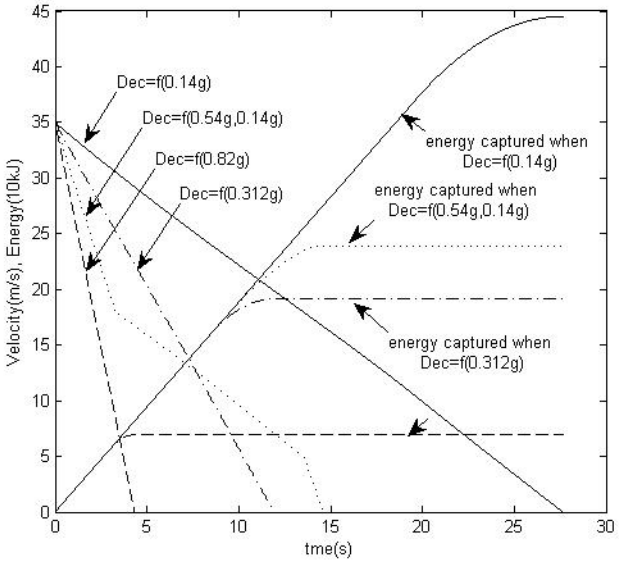

Figure 9: Summarised vehicle deceleration ratios in relation to the energy recapturing capability [12].

- The kinetic energy of the vehicle at velocity 35m/s is 735000 J

- Maximum energy that can be recaptured by the regenerative braking is 445180 J and the braking distance is 484 m

- Energy that can be captured for the minimum braking distance is 69302 J and the

braking distance is76 m

- For the braking distance of 208 m the constant braking ratio recaptures 191382 J of energy and the variable deceleration ratio recapture 239377 J of energy.

For the demanded braking distance of 208m, variable deceleration ratios capture 25% more than the energy that was captured by the constant deceleration ratio. However the time taken for the variable deceleration ratio is considerable higher than the constant deceleration ratio.

5. Experimental Verification of the Hybrid Braking System

The above mathematical modelling and simulation process has demonstrated an increase in the overall energy recovered during the regeneration process when braking with a variable deceleration (case (b)) when compared to a fixed deceleration (case (a)). In order therefore, to validate the theoretical/simulated energy storage benefits a in vehicle flywheel rig was manufactured (Figure 10). The rig allowed to simulate the vehicle mass slowing down using the flywheel system. The importance of the flywheel is critical since this allowed the investigation and decoupling of any other parasitic effects hence small differences in energy could be measured. Figure 10 shows the mechanical braking caliper experimental setup.

Corresponding Author: John Economou: *j.t.economou@cranfield.ac.uk*

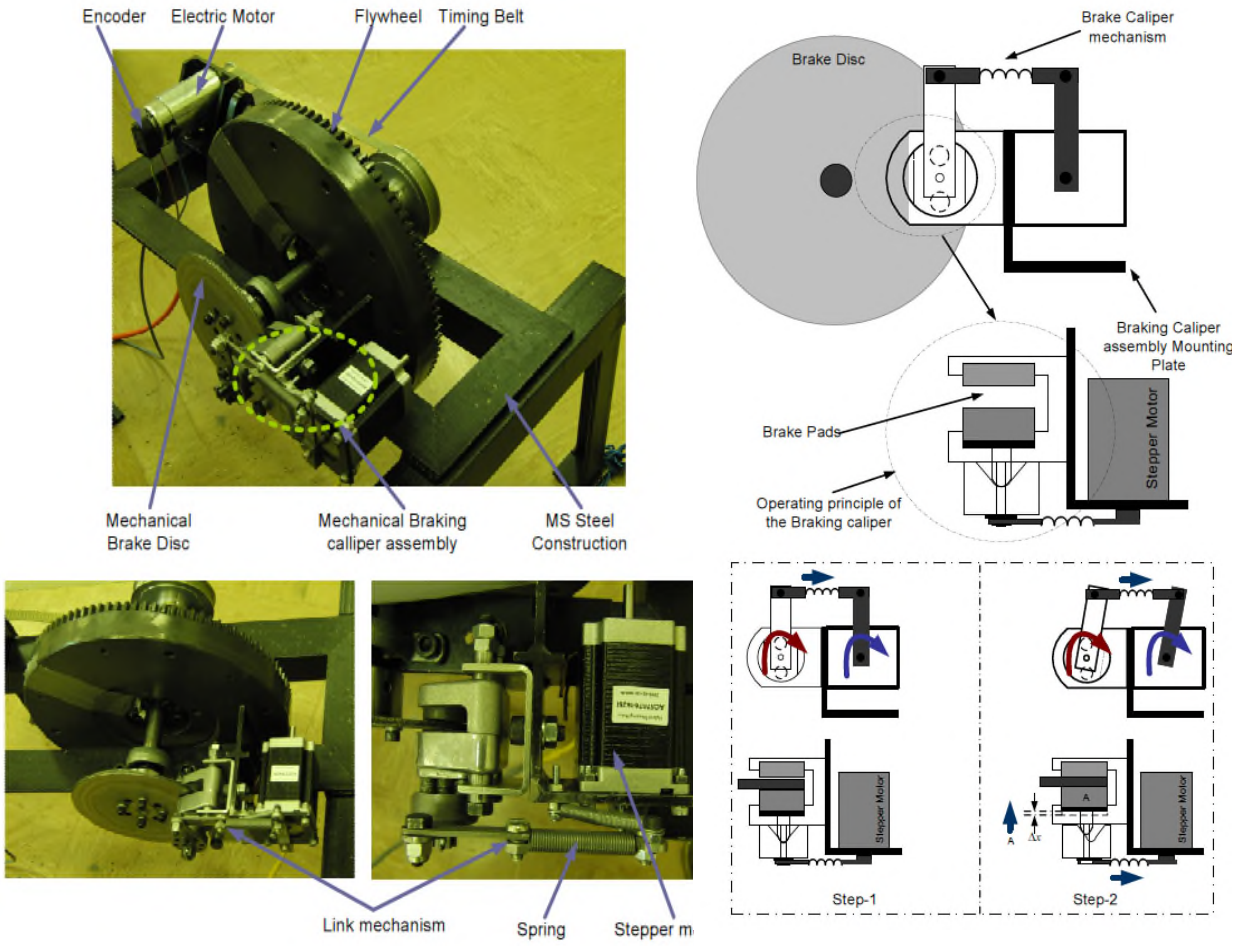

Figure 10: Electromechanical Hybrid Braking Experimental Set-up [12].

Figure 10 shows the electric motor which initially charges the flywheel at the appropriate angular velocity (to emulate the vehicle mass at speed) and then becomes the equivalent parallel hybrid motor regeneration system (energy capturing while the vehicle mass is slowing down). Kinetic energy experimental systems were also utilised in Paredes et al.[13] and Yang et al.[14] simply because these allow capturing the energy storage phenomena rather than other vehicle effects such as aerodynamics. All the experiments had the same initial vehicle kinetic energy and therefore the flywheel system had the same initial conditions. The braking started when the flywheel was at 1210 RPM.

Corresponding Author: John Economou: *j.t.economou@cranfield.ac.uk*

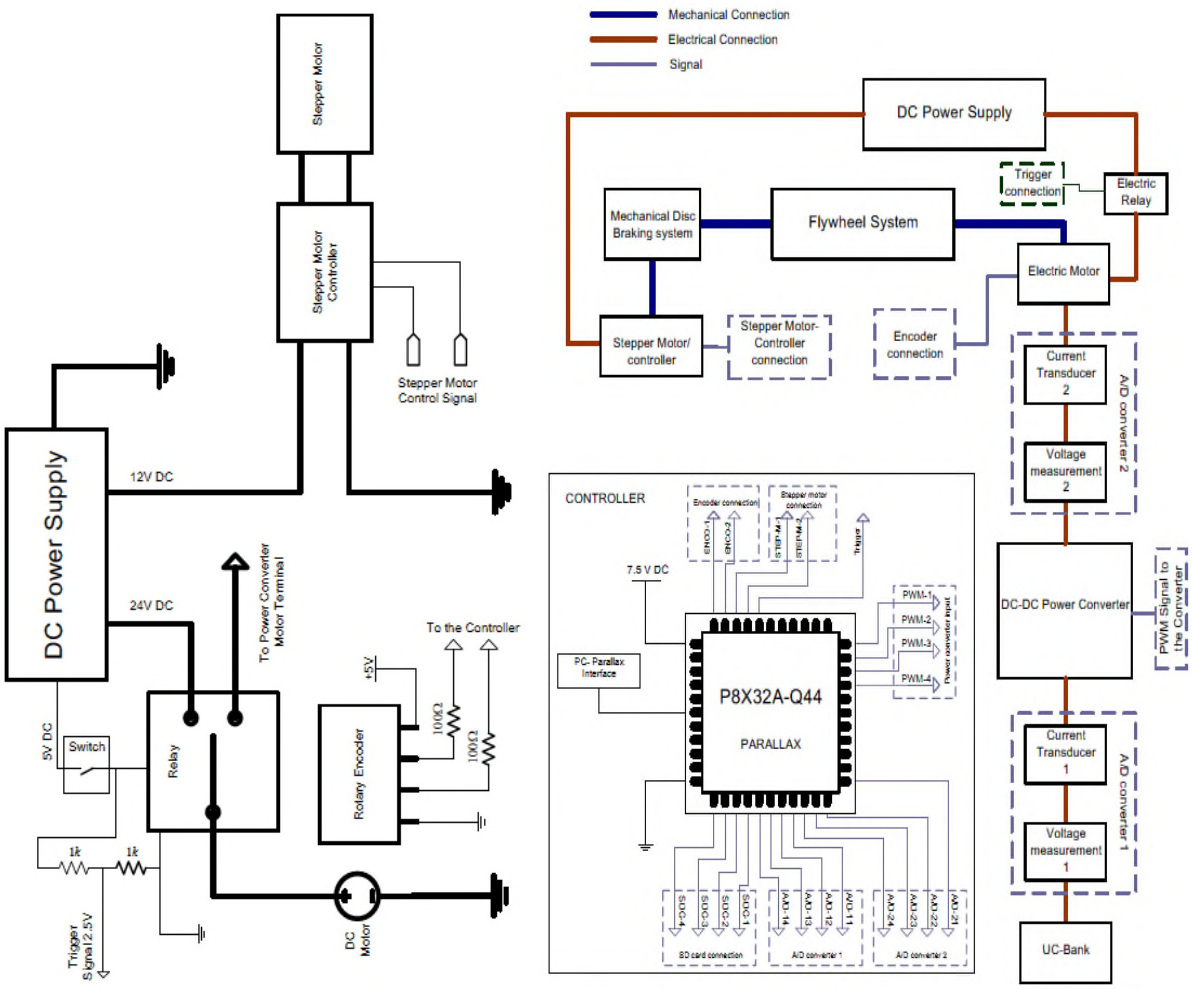

Figure 11: Power Electronics and Motion Control Experimental System [12].

A suitable stepper motor controller was utilized for the conventional brake-caliper system as shown in Figure 11 (controller). The flywheel drive motor/generator power electronics are also shown in Figure 11 together with the data acquisition unit. For the purpose of validating the extra energy capturing with the non-constant deceleration during braking two types of key scenarios were designed. One was based on constant braking torque (CBT) and one on constant braking power (CBP). For each braking scenario (CBT, CBP) three experiments were conducted showing the effects of the various dynamic vehicle and electrical variations in relation to the energy capturing. For the CBTand CBP modes of operation three torque profiles and three power profiles, respectively, were evaluated which resulted in recording the recovered energy, vehicle braking distance, vehicle velocity profile, motor voltage variation, Ultra Capacitor-bank and the duty cycle. Power buck-boost converter technologies are well discussed in Caricchi et al.[17]. The experimental set-up flowchart is shown in Figure 12 showing the process and how the various hardware systems, power electronics, flywheel, data acquisition system, power converter (drive and regeneration), conventional braking and the ultra-capacitor bank are interconnected.

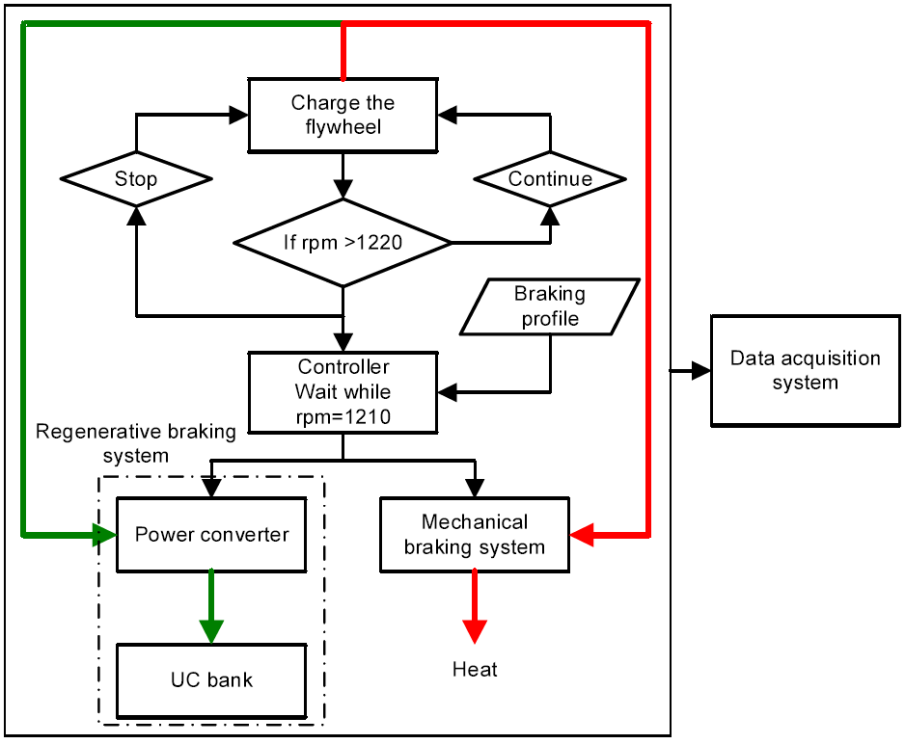

Figure 12: Experimental Rig for Measuring the excess Regeneration Energy Stored [12].

5.1. CBT, Constant Braking Torque Scenarios

Figures 13,14,15 are experimentally obtained for 455 mNm, 825 mNm, 1005 mNm maximum brake torques, respectively. In particular, Figure 13 (a) shows the speed variation and the angular displacement of the flywheel system with respect to time throughout the braking interval. Figure 13 (b) shows the braking torque distribution over the same period, where the torque due to the aerodynamic and transmission resistance as well as the regenerative braking torque.

From Figure 13 (b) the braking torque remains constant and does not exceed the 455 mNm rating. This remains the case for most of the experimental interval. After 50sec the regenerative braking torque drops until the vehicle RPM reduces to a very low level. Due to the speed variation and internal resistance of the electric motor, sufficient back-emf could not be produced by the motor to generate the predefined torque below the speed of 100 rpm for this test. Although the flywheel (vehicle mass) slows down due to the regeneration process however also the torque due to the aerodynamic and transmission resistance both contribute to the braking process.

Figure 13 (c) illustrates the current flow rate of the electric motor and UC-bank. Clearly the braking torque

due to regeneration follows a similar pattern to that of the motor/generator current. The total energy stored in the flywheel at the experimental start-up instant for this braking scenario, and consequently the recovered energy, are depicted in Figure 13 (c) and Figure 13 (d). 55% of the stored energy is recovered in the UC-bank in this braking scenario. UC banks were also used in Paredes et al.[13] in association with a battery system as well. However in Paredes et al.[13] the paper focuses on combined braking for the case of an induction machine rather the DC motor that is used in the topology discussed in the present paper. Furthermore this paper focuses towards extending the braking duration thus increasing the energy captured from the kinetic regeneration process. Other researchers also considered for the kinetic energy system an induction machine, however a more intelligent-based method was applied Cholula et al.[16]. Figure 13 (e) shows the terminal voltage of the electric motor and UC-bank. The back-emf of the electric motor is also shown. From Figure 13(e) the EM terminal voltage and the back-emf are different, mainly due to internal voltage drop inside the electric motor, which is eventually dissipated as heat due to the internal resistance.

Figure 13 (f) illustrates the variation of the power converter's duty cycle value with respect to time. After 50sec, when the duty cycle value reaches 100% in boost mode operation, there is no current flow into the UC-bank and the electric motor is short circuited. Therefore all the available energy in the flywheel system after this point is simply dissipated as heat in the internal resistance of the electric motor and in the transmission system.

Case (A1): Experimental Results A1 – Constant Braking Torque Scenario ($455x10^{-3}Nm$)

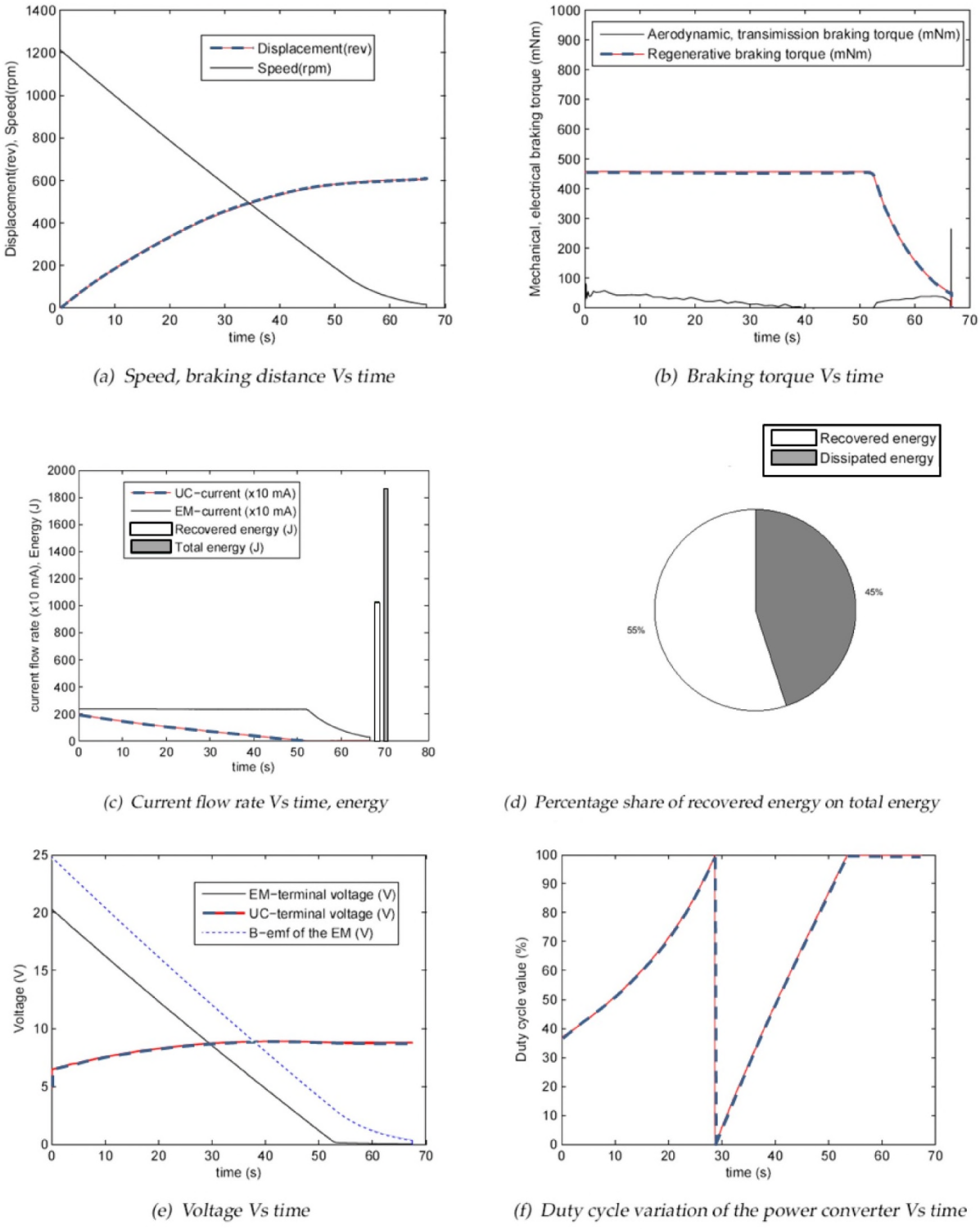

(a) Speed, braking distance Vs time

(b) Braking torque Vs time

(c) Current flow rate Vs time, energy

(d) Percentage share of recovered energy on total energy

(e) Voltage Vs time

(f) Duty cycle variation of the power converter Vs time

Figure 13: Constant Torque Braking 455mNm Experimental Results [12].

Case (A2): Experimental Results A2 – Constant Braking Torque Scenario ($825x10^{-3}Nm$)

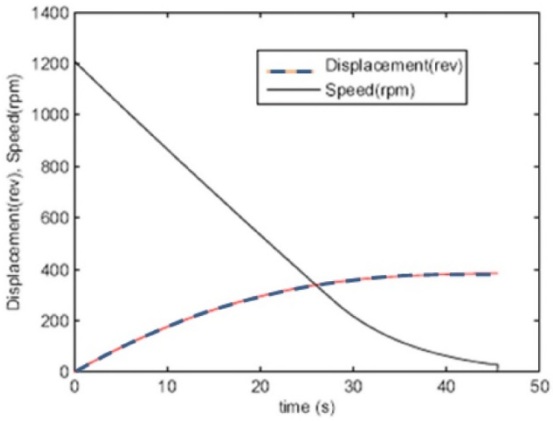

(a) Speed, braking distance Vs time

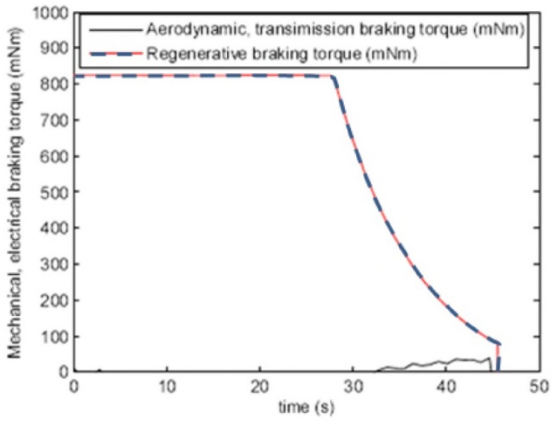

(b) Braking torque Vs time

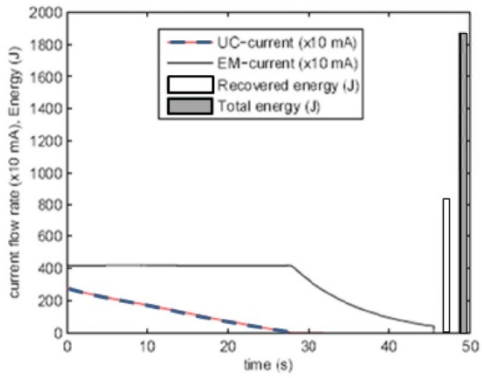

(c) Current flow rate Vs time, energy

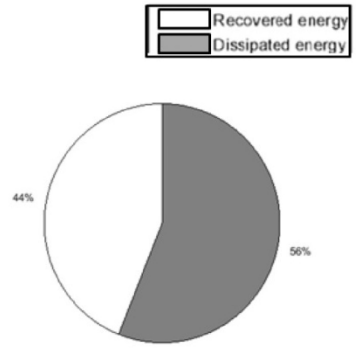

(d) Percentage share of recovered energy on total energy

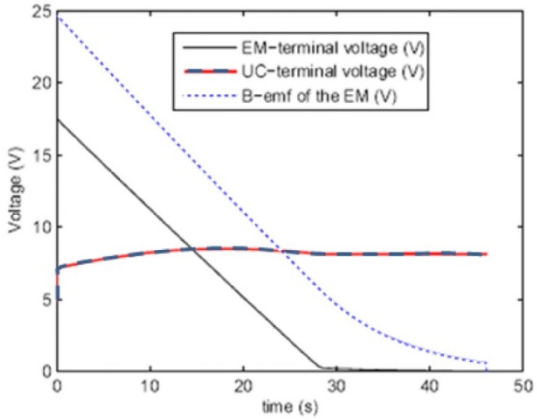

(e) Voltage Vs time

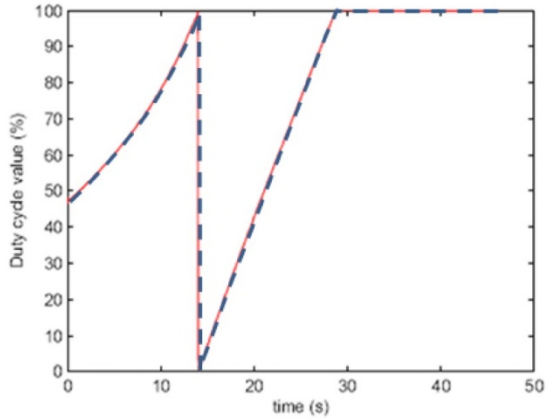

(f) Duty cycle variation of the power converter Vs time

Figure 14: Constant Torque Braking 825mNm Experimental Results [12].

Case (A3): Experimental Results A3 - Constant Braking Torque Scenario (1005x *Nm*)

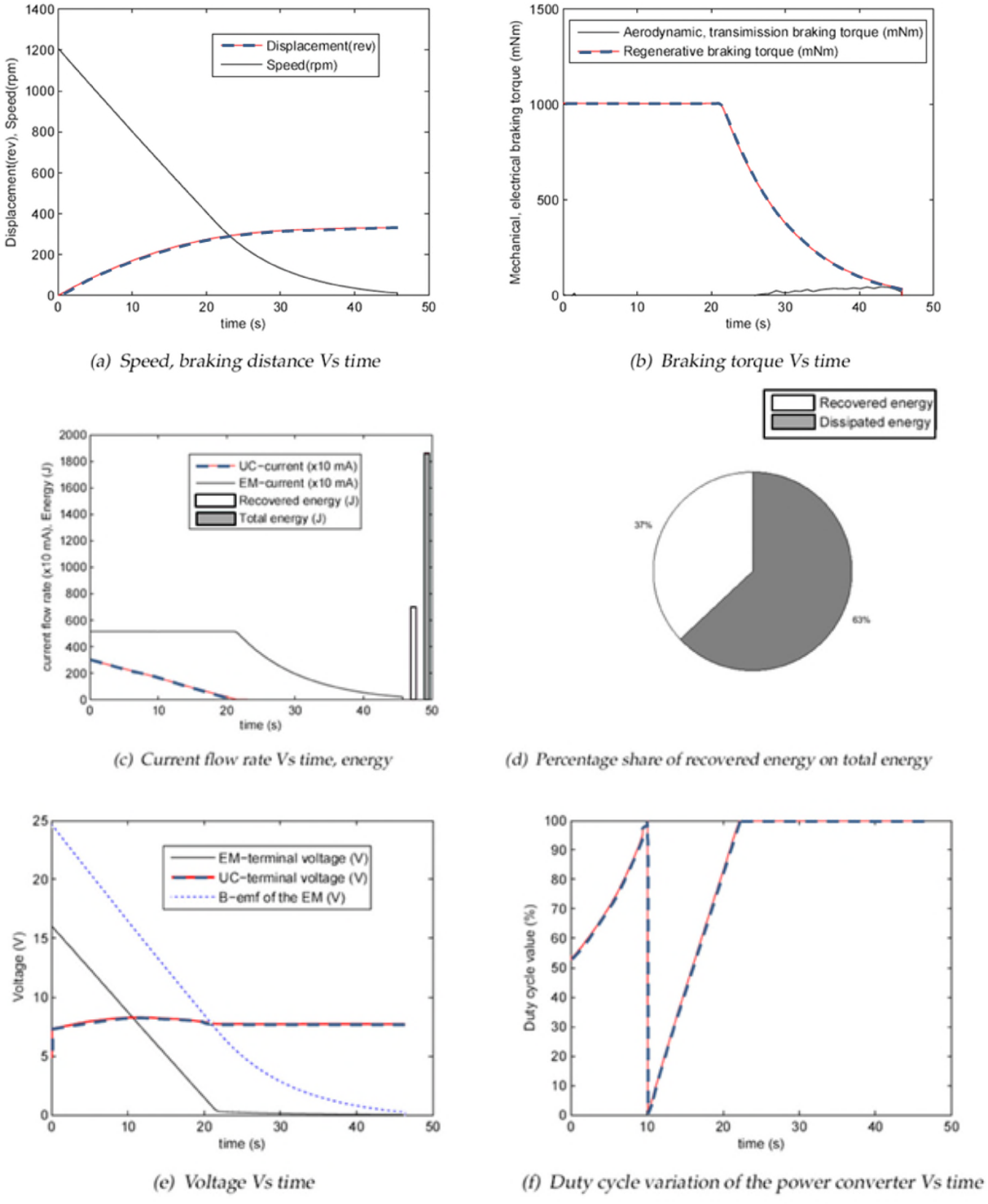

(a) Speed, braking distance Vs time

(b) Braking torque Vs time

(c) Current flow rate Vs time, energy

(d) Percentage share of recovered energy on total energy

(e) Voltage Vs time

(f) Duty cycle variation of the power converter Vs time

Figure 15: CBT 1005mNm Experimental Results [12].

Similarly, results shown in Figures 14 and 15 demonstrate that the current increase (due to the increasing braking torque) has affected the kinetic energy recovery process. Hence it should be noticed from these results that increasing the current significantly affects the kinetic energy recovery of the flywheel system. From Figures 13,14,15 we can conclude that high braking torques are not desirable in relation to the vehicle kinetic energy [12].. A further observation is that when at the end of the experiments the duty-cycle becomes 100% then the power converter has its controllability limit whereby the mechanical stepper motor caliper system is required to smoothly engage.

5.2. CBP, Constant Braking Power Scenarios

This specific experimental scenario leads towards a better understanding of the issues relating to a constant power flow rate. The results obtained from the constant braking power are then compared to the results obtained from the constant braking torque. The initial conditions are identical to the ones applied to the constant braking torque scenarios. The braking motor torque was varied by modifying the reference duty cycle of the power converter in relation to the flywheel speed variation. Similarly to the previous scenarios the recorded data included: the recovered energy, braking distance, velocity profile, torque profile, motor voltage variation, UC-bank and the duty cycle variation.

Figure 16 shows the results obtained for a 30W constant braking power scenario. As shown in Figure 16 (a) and (b) a constant braking power scenario produces an uneven braking torque and velocity profile. Although this may be acceptable electrically it would normally be considered as inappropriate for the passengers within a vehicle because of comfort issues; this is not a concern, however, for an unmanned vehicle.

Corresponding Author: John Economou: *j.t.economou@cranfield.ac.uk*

Case (B1): Experimental Results B1 - Constant Braking Power Scenario (*30W*)

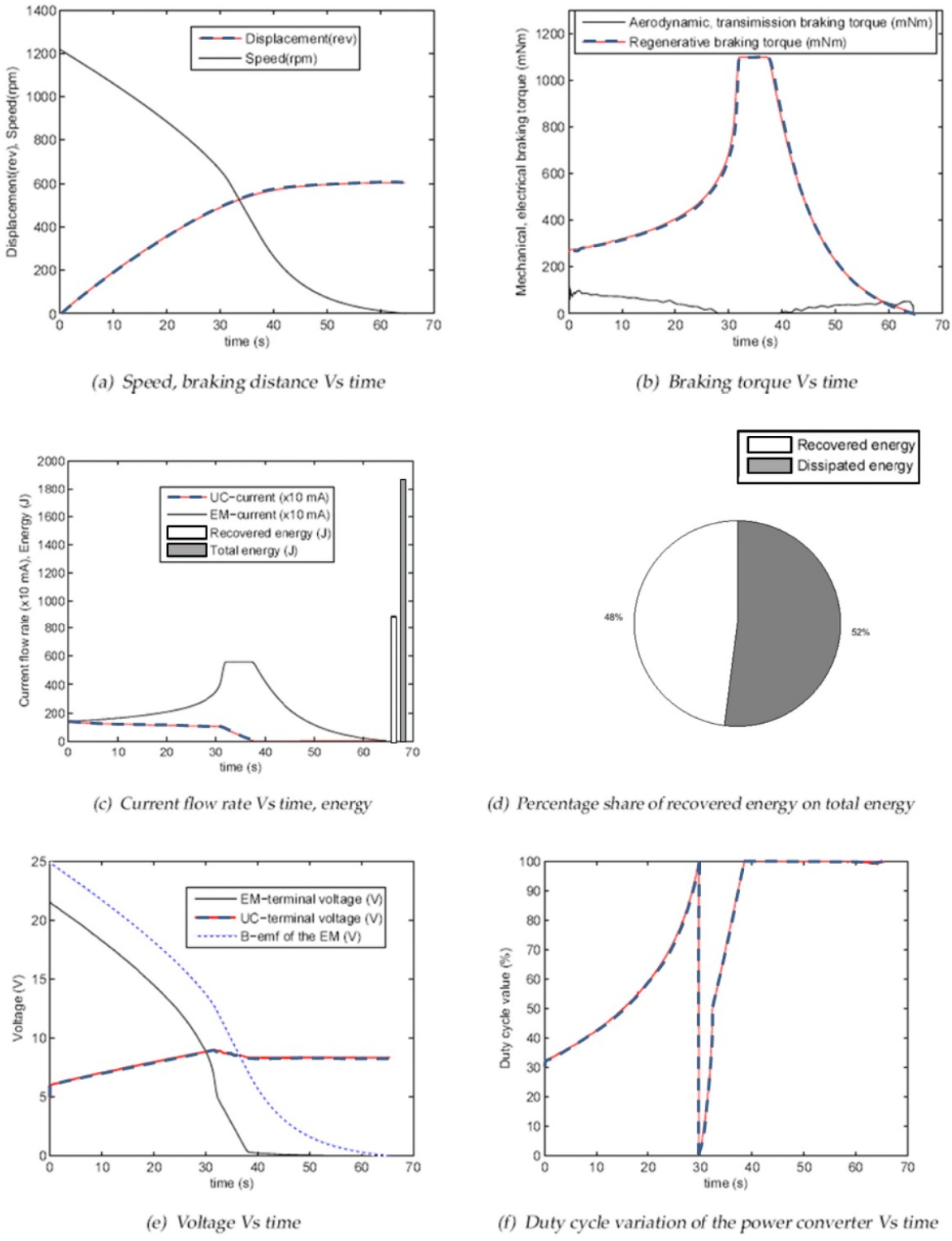

(a) Speed, braking distance Vs time

(b) Braking torque Vs time

(c) Current flow rate Vs time, energy

(d) Percentage share of recovered energy on total energy

(e) Voltage Vs time

(f) Duty cycle variation of the power converter Vs time

Figure 16: Constant Braking Power 30W Experimental Results [12].

Case (B2): Experimental Results B2 - Constant Braking Power Scenario (*65W*)

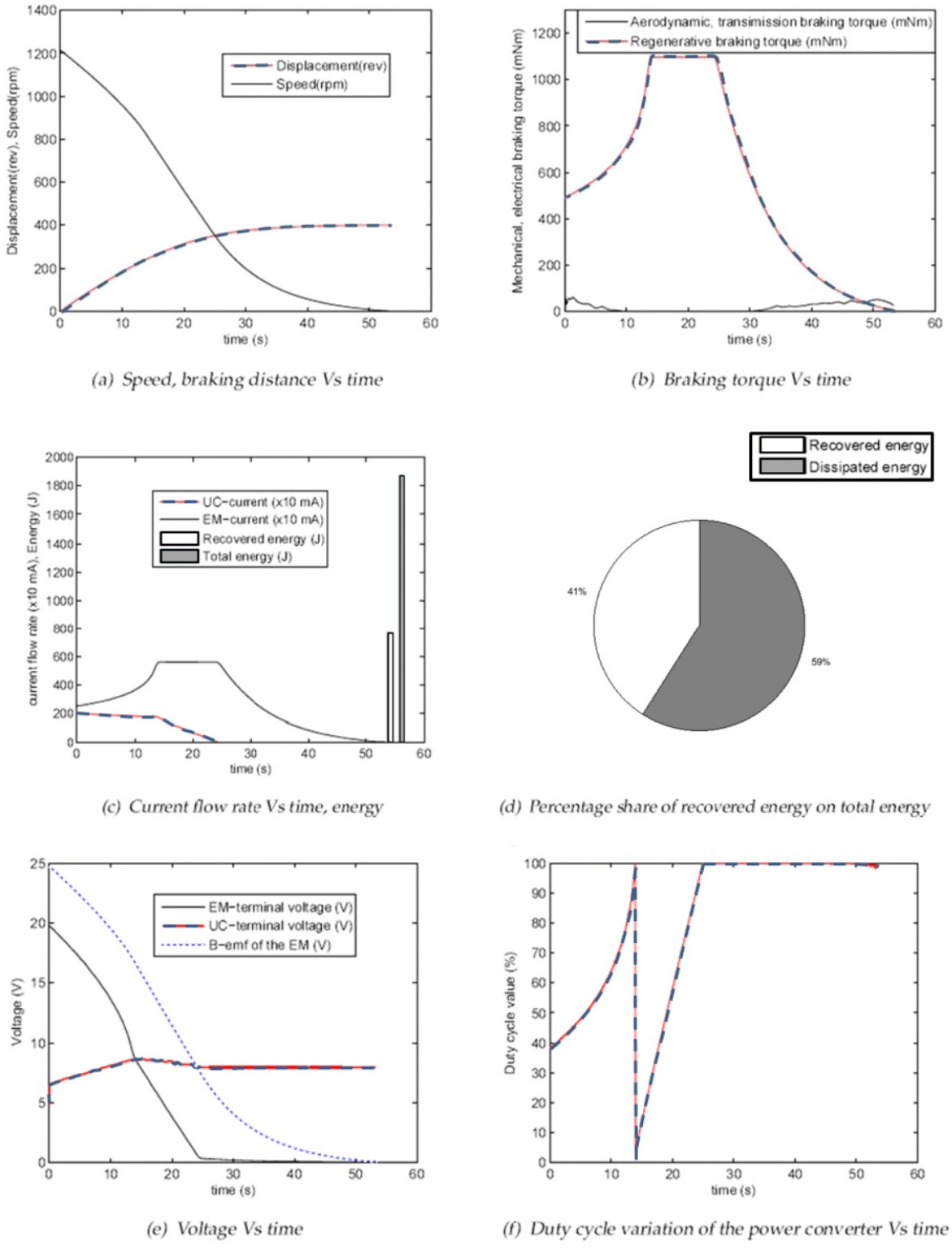

(a) Speed, braking distance Vs time

(b) Braking torque Vs time

(c) Current flow rate Vs time, energy

(d) Percentage share of recovered energy on total energy

(e) Voltage Vs time

(f) Duty cycle variation of the power converter Vs time

Figure 17: Constant Braking Power 65W Experimental Results [12].

Case (B3): Experimental Results B3 - Constant Braking Power Scenario (*96W*)

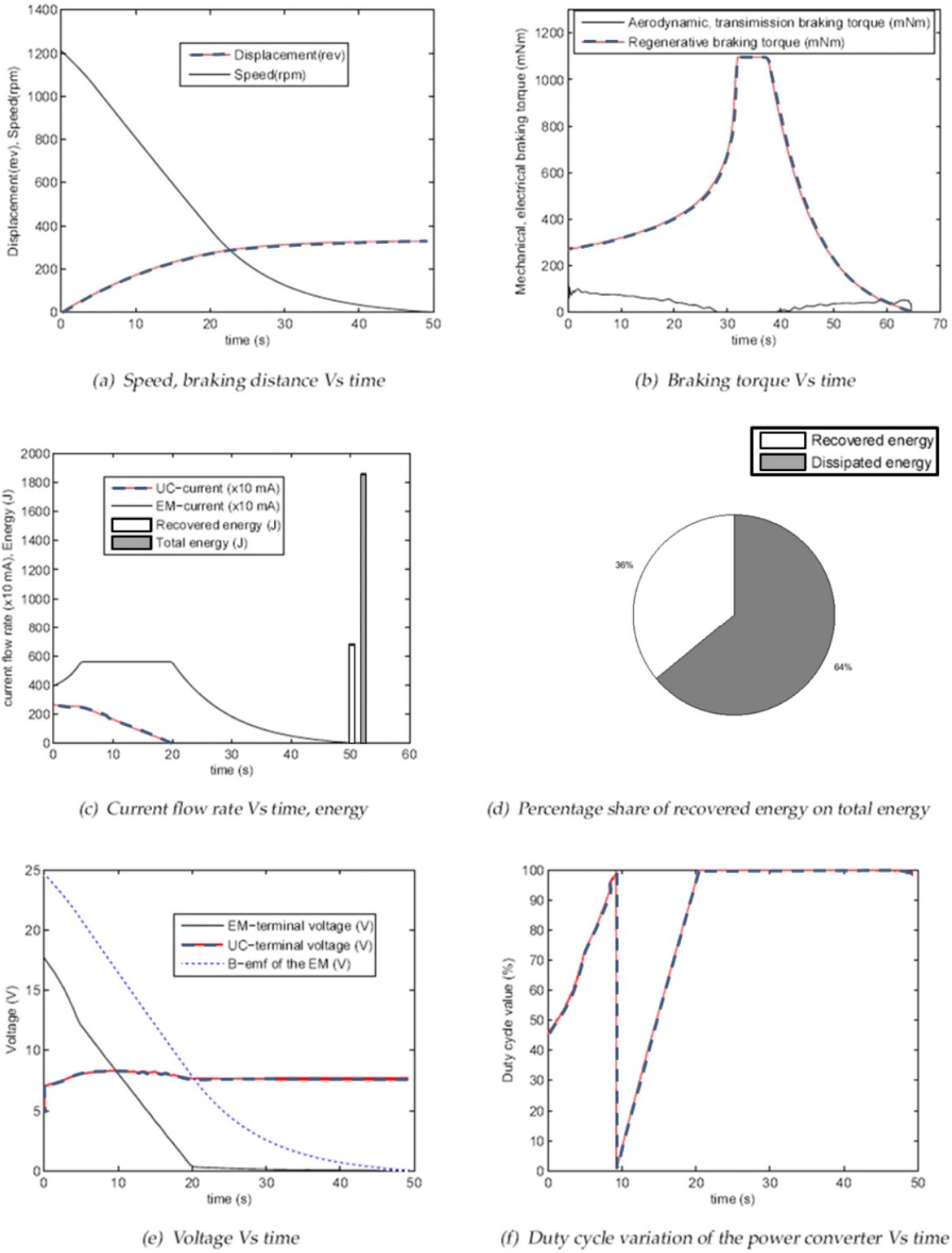

(a) Speed, braking distance Vs time

(b) Braking torque Vs time

(c) Current flow rate Vs time, energy

(d) Percentage share of recovered energy on total energy

(e) Voltage Vs time

(f) Duty cycle variation of the power converter Vs time

Figure 18: CBT 96W Experimental Results [12].

In summary, the experimental results from both categories A (Constant Braking Torque, CBT) and B (Constant Braking Power, CBP) have been summarized in Table 3. The table represents the comparisons of the two different braking methods and the effective kinetic energy recovered with respect to the braking distance.

CBT(*mNm*)	% Energy	CBP(*W*)	% Energy	Braking distance
455 *mNm*	55%	30 *W*	48 %	600 *rev*
825 *mNm*	44%	65 *W*	41 %	400 *rev*
1005 *mNm*	37%	96 *W*	36 %	320 *rev*

Table 3: Constant Braking Torque and Constant Braking Power Algorithm Energy Based

Experimental Comparisons

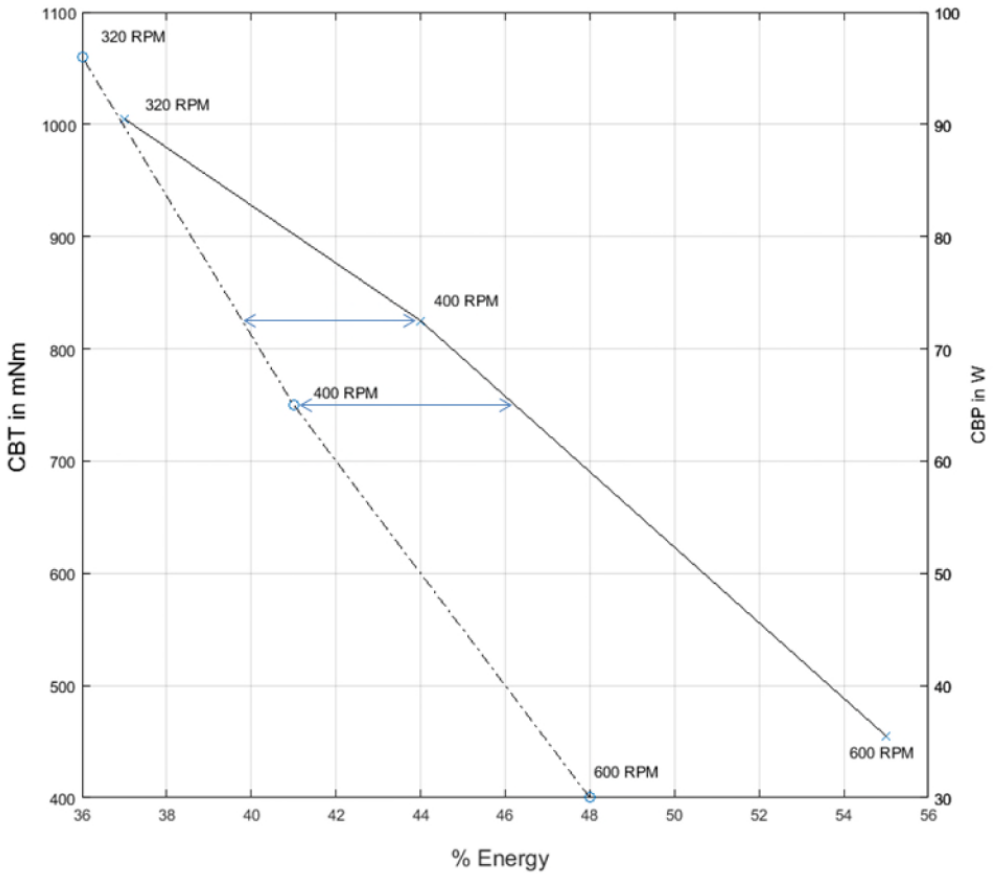

Figure 19 Energy Based Summary of Comparisons of CBT versus CBP braking methods.

In Figure 19 the CBT (solid line) and CBP (dashed line) are shown in relation to the percent recovered energy and the equivalent distance to brake the vehicle (in RPM, thus wheel-size independent). Both braking methods/algorithms perform well and result in energy recovery. However, the CBT method

performs better than the CBP method and also is more practical in terms of user acceptance. The paper

has focused on the detailed braking effects rather than the effects in relation to a standard driving cycle because these are more suited for emissions testing. Hence, the experiments in the paper are run for these specific test conditions so that the braking effects can be analysed in relation to the energy recovery braking algorithms. The experimental results for both braking regimes showed that the constant torque braking is more efficient for kinetic energy recovery than constant power braking.
Passenger comfort is not a concern because the class of vehicles for which the proposed braking strategy is applicable is unmanned land vehicles when used in public roads (delivery and general purpose utility vehicles for example). In addition to that, the velocity profile of the constant torque braking scenario is more linear and controllable than the constant power braking regime. In summary based on the results shown and also Suntharalingham et al.[15] the following conclusions were drawn from the constant torque, constant power braking experiments

•Higher braking torque reduces the kinetic energy recovery of the drivetrain compared with lower braking torques.

•Since constant braking power includes a range of current flow rates throughout the braking process and constant braking torque maintains consistency of current flow rate, constant braking torque is desirable to increase the kinetic energy recovery for a given braking requirement (braking distance).

•Constant braking torque results in a more controllable and uniform deceleration profile than the constant braking power regime. In practical terms, there are braking scenarios which require the regenerative braking system to operate together with the caliper braking system. Therefore, a combination of regenerative braking and secondary braking systems should be engaged to fulfil these braking requirements.

6. CONCLUSIONS

The theoretical results have demonstrated that extending the braking time while satisfying the vehicle constraints for a set braking distance has resulted in a novel braking strategy for the category of unmanned parallel hybrid power train configurations when used in public roads. The method proposed enhances the regenerative energy capturing ability while utilizing both the electric motor as brake and a conventional caliper brake system. Since the demanded braking requirement will vary according to the driving circumstances, there is an infinite number of braking ratios which could be

explored. However, because this was not practical to explore, the proposed algorithm was focused towards a set of moderate variable deceleration ratios. This has extended the braking time period while maintaining the same braking distance and allowed the motor generator to recapture more energy than other braking strategies that only have a constant deceleration ratio. Although the proposed algorithm may have limitations in use for passenger cars, it is very practical for use for unmanned land vehicles used in public roads. The reason is that passenger comfort is not anymore a design constraint and therefore the algorithm can be tuned with energy savings as its prime priority. The experimental results have compared two different braking methods and explored their relative benefits. Furthermore, it can be extrapolated that many single braking events will occur per day, thus resulting in multiple and accumulative energy braking savings. The reason that this paper focused on the single braking events is that the algorithms (CBT, CBP) can be explored and assessed. The constant braking torque (CBT) strategy overall has indicated a more superior energy capturing ability when compared to the Constant Braking Power (CBP) strategy for the class of unmanned land vehicles when used in public roads whereby energy capturing (is important for the vehicle) and braking distance is key to pedestrian safety (minimum distance for braking).

Corresponding Author: John Economou: *j.t.economou@cranfield.ac.uk*

NOMECLATURE

a	Vehicle deceleration
μ	Terrain adhesive coefficient
F_b	Vehicle wheels braking force
T_b	Braking torque applied to the wheels
I	Wheel inertia
α_{an}	Wheel angular acceleration
r	Rolling wheel radius
F_{res}	Resulting braking force
f_r	Rolling resistance
W	Vehicle weight
θ_s	Road angle of inclination
R_a	External force acting on the vehicle
W_f	Normal acting on front axle
L	Longitudinal distance between front and rear axle
l_2	Length of rear axle to vehicle CG
h	Vertical distance from ground to vehicle CG
W_r	Normal load acting on rear axle
l_1	Length of front axle to vehicle CG
F_{bf}	Braking force acting on the front wheels
F_{br}	Braking force acting on the rear wheels
$F_{generator}$	Force captured by the electric motor/generator mode
$v(t)$	Velocity of vehicle (final)
t	Time independent variable
M	Vehicle mass
F_a	External force acting on vehicle
F_g	External force acting on vehicle
k_1	Weight for deceleration ratio for mechanical braking
F_{mech}	Force associated with mechanical braking
k_2	Weight for deceleration ratio for electrical braking
F_{motor}	Force associated with electrical braking
OF	Other factors (non modelled)
$V_{t=t_s}$	Vehicle velocity at time t_s
OE	Other energy associated to OF
E_{regn}	Regeneration energy
P_{regn}	Motor regeneration power
U	Initial vehicle velocity
i	Road section index
KE	Kinetic energy
E_{others}	Energy for non-modelled minor phenomena
t_f	Final time per section

Corresponding Author: John Economou: *j.t.economou@cranfield.ac.uk*

t_s	Start time per section
Δt	Small time interval
P_{others}	Power corresponding to E_{others}
P_{mech}	Mechanical brake power
T	Overall braking time interval
n	Number of equally timed section
t_1	First interval i.e. $n = 1$
t_2	Second interval i.e. $n = 2$
t_i	General case for $i = 1,2,3, \ldots i$
$S_{braking}$	Vehicle braking distance
$s(t)$	Distance travelled by vehicle for each i section
S	Demanded braking distance
$B\_P_{position}$	Brake pedal position
$SoC_{energy\ storage}$	Energy storage state of charge
$V_{vehicle}$	Current vehicle velocity
$B\_Torque(t)$	Braking torque
$k(t)$	Percentage of mechanical torque
Me_T_{max}	Braking torque
Dec	Deceleration
Brk	Brake
UC	Ultra-capacitors
EM	Electric motor
B_emf	Back electromotive force

REFERENCES

1. Shuang G., Chau K.T., Chunhua L., Diyun W., Chan C.C. Integrated Energy management of Plug-in Electric Vehicles in Power Grid With Renewables. *IEEE Transactions on Vehicular Technology* 2014; 63: 3019 – 3027.

2. Khaligh A., Zhihao L., Battery, Ultracapacitor, Fuel Cell, and Hybrid Energy Storage Systems for Electric, Hybrid Electric, Fuel Cell, and Plug-In Hybrid Electric Vehicles: State of the Art. *IEEE Transactions on Vehicular Technology* 2010; 59: 2806 - 2814.

3. Zhang G. Research of the regenerative braking and energy recovery system for electric vehicle. In: *(WAC) World Automation Congress* ,PuertoVallarta,Mexico,24-28June 2012, pp.1-4. NJ: IEEE.

4. Wang F., Zhuo B. Regenerative braking strategy for hybrid electric vehicles based on regenerative torque optimization control. *Proceedings IMechE Part D: Journal Automobile Engineering* 2008; 222: 499-513.

5. Yeo H., Kim H., Hardware in loop simulation of regenerative braking for a hybrid electric vehicle. *Proceedings IMechE Part D: Journal of Automobile Engineering* 2002; 216: 855-864.

6. Bhangu B.S.,Bentley P., Stone D.A. , Bingham C.M. Nonlinear Observers for Predicting State-of-Charge and State-of-Health of Lead-Acid Batteries for Hybrid-Electric Vehicles. *IEEE Transactions on Vehicular Technology* 2005; 54: 783 - 794.

7. Panagiotidis M., Delagrammatikas G., Assanis D. Development and use of a regenerative braking model for a parallel hybrid electric vehicle. In: *SAE Technical Paper Series,* Detroit, Michigan, 6-9 March 2000. USA: SAE.

8. Wong J.Y. *Theory of ground vehicles*,2nd ed. John Wiley & Sons, 1993.

9. Miller J.M. *Propulsion system for hybrid vehicles*. IET Power & Energy Series 45, 2004.

10. Mi C., Lin H., Zhang Y. Iterative learning control of antilock braking of electric and hybrid vehicles. *IEEE Transaction on Vehicular Technology* 2005; 54: 486 - 494.

11. Bray J.T., Walker G. R., Simpson A. G., Greaves M. C., Guymer B. D. Braking system performance requirements of a lightweight electric/ hybrid rear wheel drive vehicle.

Corresponding Author: John Economou: *j.t.economou@cranfield.ac.uk*

International Journal Vehicle Autonomous Systems 2003; 1: 436 - 448.

12. Suntharalingam P. *Kinetic Energy Recovery and Power Management for Hybrid Electric Vehicles.* PhD Thesis, Cranfield University, UK, 2011.

13. Paredes, M.G.S.P., Pomilio J.A., Santos A.A. Combined regenerative and mechanical braking in electric vehicle. In: *COBEP Power Electronics Conference*, Gramado, Brazil, 27-31 October 2013, pp.935–941. NJ: IEEE.

14. Yang X. Nonlinear model of a flywheel vehicle. In: (EMEIT) *Electronic and Mechanical Engineering and Information Technology*, Harbin, 12-14 August 2011, Heilongjiang, pp. 3615–3617. NJ: IEEE.

15. Suntharalingam P., Economou J.T., Knowles K. Effect on Regenerative Braking Efficiency with Deceleration Demand and Terrain Condition. In: *PEMD Power Electronics, Machines and Drives*, Brighton, UK, 19-21 April 2010, pp.1-6. London: IET.

16. Cholula S., Claudio A., Ruiz J. Intelligent control of the regenerative braking in an induction motor drive. In: *2nd ICEEE International Conference on Electrical and Electronic Engineering (ICEEE) and XI Conference on Electrical Engineering*, Mexico City, Mexico. 7-9 September 2005, pp.302-308. NJ: IEEE.

17. Caricchi F., Crescimbini F., Giulii Capponi F., Solero L. Study of bi-directional buck-boost converter topologies for application in electrical vehicle motor drives. In: *APEC Applied Power Electronics Conference and Exposition*, Anaheim, California, 15-19 February 1998, pp.287-293 vol.1. NJ: IEEE.

18. CS Nanada Kumar, Shakar C Subramanian, "Cooperative control of regenerative braking and friction braking for a hybrid electric vehicle", *Proceedings of the Institution of Mechanical Engineers, Part D: Journal of Automobile Engineering*, January 2016; vol. 230, 1: pp. 103-116., first published on April 19, 2015.

Corresponding Author: John Economou: *j.t.economou@cranfield.ac.uk*

Kinetic energy storage using a dual braking system for unmanned parallel hybrid electric vehicle

Suntharalingam, Piranavan

2016-11-06

Suntharalingam P, Economou JT, Knowles K. (2016) Kinetic energy storage using a dual braking system for unmanned parallel hybrid electric vehicle. Proceedings of the Institution of Mechanical Engineers, Part D: Journal of Automobile Engineering, Volume 231, Issue 10, September 2017, pp.1353-1373

https://doi.org/10.1177/0954407016672591